

LOCKHEED MARTIN ENERGY RESEARCH LIBRARIES



3 4456 0515455 1

CENTRAL RESEARCH LIBRARY

ORNL-4868

cy. 2

MEASUREMENT OF  
SHOCK OVERPRESSURE IN AIR BY A  
YIELDING FOIL MEMBRANE BLAST GAUGE

R. W. Manweiler  
C. V. Chester  
C. H. Kearny

OAK RIDGE NATIONAL LABORATORY  
CENTRAL RESEARCH LIBRARY  
DOCUMENT COLLECTION

**LIBRARY LOAN COPY**

DO NOT TRANSFER TO ANOTHER PERSON

If you wish someone else to see this  
document, send in name with document  
and the library will arrange a loan.

UCN-7969  
(3 3-67)



**OAK RIDGE NATIONAL LABORATORY**

OPERATED BY UNION CARBIDE CORPORATION • FOR THE U.S. ATOMIC ENERGY COMMISSION

Printed in the United States of America. Available from  
National Technical Information Service  
U.S. Department of Commerce  
5285 Port Royal Road, Springfield, Virginia 22151  
Price: Printed Copy \$4.00; Microfiche \$0.95

This report was prepared as an account of work sponsored by the United States Government. Neither the United States nor the United States Atomic Energy Commission, nor any of their employees, nor any of their contractors, subcontractors, or their employees, makes any warranty, express or implied, or assumes any legal liability or responsibility for the accuracy, completeness or usefulness of any information, apparatus, product or process disclosed, or represents that its use would not infringe privately owned rights.

Contract No. W-7405-eng-26

Civil Defense Research Section  
HEALTH PHYSICS DIVISION

MEASUREMENT OF SHOCK OVERPRESSURE IN AIR  
BY A YIELDING FOIL MEMBRANE BLAST GAUGE

by

R. W. Manweiler, C. V. Chester and C. H. Kearny

SEPTEMBER 1973

OAK RIDGE NATIONAL LABORATORY  
Oak Ridge, Tennessee 37830  
operated by  
UNION CARBIDE CORPORATION  
for the  
U. S. ATOMIC ENERGY COMMISSION

LOCKHEED MARTIN ENERGY RESEARCH LIBRARIES

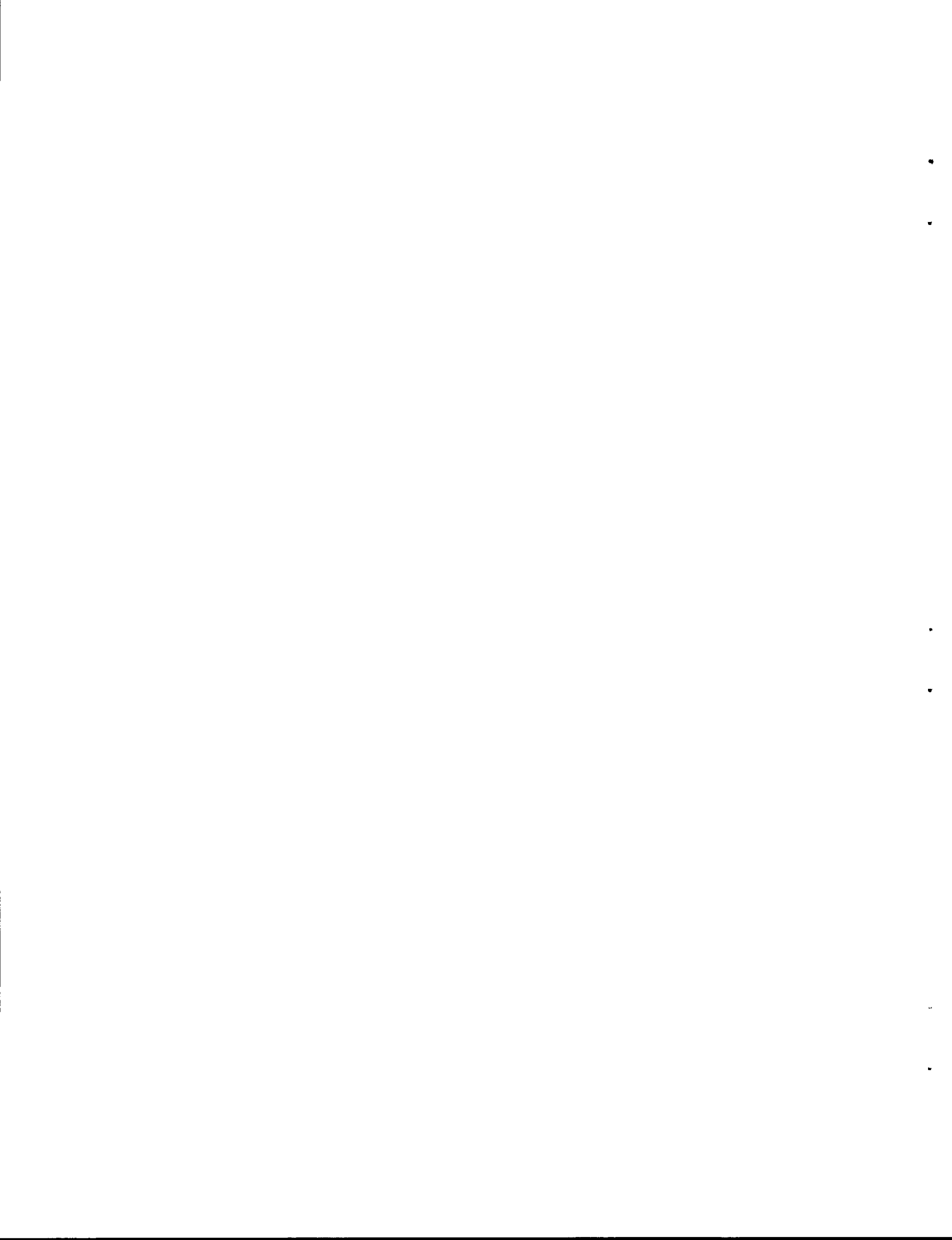


3 4456 0515455 1



## CONTENTS

	<u>Page</u>
LIST OF FIGURES . . . . .	iv
ABSTRACT . . . . .	1
I. INTRODUCTION . . . . .	2
II. THEORY OF FOIL MEMBRANES . . . . .	2
III. CALIBRATION OF FOIL MEMBRANES . . . . .	4
IV. THE DESIGN OF THE GAUGE . . . . .	12
A. General Description . . . . .	12
B. Choosing D and T . . . . .	19
C. Other Membrane Gauges . . . . .	20
V. THE EXPERIMENTAL FIELD RESULTS . . . . .	20
VI. CONCLUSIONS AND RECOMMENDATIONS . . . . .	26
REFERENCES . . . . .	27



## LIST OF FIGURES

	<u>Page</u>
Fig. 1. Stress-strain curve for 0.005-inch-thick aluminum foil . . .	6
Fig. 2. Stress-strain curves for 0.005- and 0.001-inch-thick aluminum foil . . . . .	7
Fig. 3. Pressure as a function of permanent deformation for 0.005-inch-thick aluminum foil . . . . .	8
Fig. 4. Pressure as a function of permanent deformation for 0.001-inch-thick aluminum foil . . . . .	9
Fig. 5. Pressure as a function of time curves for short and long duration shock tube pulses . . . . .	11
Fig. 6. Mechanical drawing (side view) of pressure gauge . . . . .	13
Fig. 7. Assembled gauge of the dimensions given in Fig. 6, and a smaller (6-in.) gauge shown partially disassembled . . . .	14
Fig. 8. Pressure gauge mounted to measure the ground-surface overpressure with protective plate removed . . . . .	15
Fig. 9. Pressure gauge mounted to measure the ground-surface overpressure with protective plate in place . . . . .	16
Fig. 10. Top view of membrane plate with 0.005-inch-thick foils after subjection to 15 psi nominal overpressure . . . . .	17
Fig. 11. Bottom view of membrane plate with 0.005-inch-thick foils after subjection to 15 psi nominal overpressure . . .	18
Fig. 12. Recorded overpressures compared with predicted pressure-distance curve (Ref. 4). The ORNL membrane- gauge experimental readings are shown as shaded symbols. The transducer readings of Refs. 7 and 8 are shown as unshaded symbols, for comparison. A 10% uncertainty was assigned to the transducer readings . . . . .	25

MEASUREMENT OF SHOCK OVERPRESSURE IN AIR BY  
A YIELDING FOIL MEMBRANE BLAST GAUGE

R. W. Manweiler, C. V. Chester and C. H. Kearny

ABSTRACT

An inexpensive yet accurate pressure gauge was designed making use of the relationship between the peak pressure of a single-step rise shock loading and the permanent plastic deformation of thin foil membranes when subjected to shock loading. The gauge is of extremely simple design, is easy to use, and requires no electronic equipment. Peak shock overpressures from a few psi to hundreds of psi can be measured to about 10% accuracy. The relevant theory of shock loading of thin foil membranes is presented, the calibration procedure using a shock tube is given, and the results of experimental field tests are given and compared to standard shock overpressure measurements.

## I. INTRODUCTION

An inexpensive yet accurate pressure gauge was designed making use of the relationship between the peak pressure of a single-step rise shock loading and the permanent plastic deformation of thin foil membranes when subjected to shock loading. The gauge is of extremely simple design, is easy to use, and requires no electronic equipment. Peak shock overpressures from a few psi to hundreds of psi can be measured to about 10% accuracy and the cost of the gauge is only a few percent of the cost of a transducer-electronic channel gauge. The gauge has been successfully field tested in a realistic experimental environment. The gauge is not calibrated for multiple step shocks or slowly rising pressure.

In Section II the relevant theory of thin foil membranes is presented and in Section III the calibration experiments for aluminum foil membranes are discussed. Section IV contains the design of the gauges, Section V discusses the results of experimental field tests and, finally, Section VI summarizes this work.

## II. THEORY OF FOIL MEMBRANES

The permanent plastic deformation of circular foils subjected to shock loading was calculated by Dresner.<sup>1</sup> He showed that for a shock wave of instantaneous risetime and of infinite duration with normal incidence upon a circular foil membrane, the stress  $\sigma$  and incident pressure  $P$  (both measured in psi) are related by

$$\frac{\sigma}{P} = .138 \frac{(D/T)^2}{(h/T)} \quad (1)$$

$D$  is the membrane's diameter (in inches),  $T$  is the thickness (in mils) and  $h$  is the maximum permanent deformation of the foil membrane (in inches). The symbols  $P$ ,  $D$ ,  $h$ ,  $T$ ,  $\sigma$ , and  $\eta$  will be henceforth used to represent the pressure, membrane diameter, deformation, membrane thickness, stress, and average linear strain, respectively. Eq. (1) was derived by Dresner<sup>1</sup>

assuming first that the elastic limit of the foil occurs at a negligibly small strain, and second that the stress was constant in the plastic region. He also experimentally tested Eq. (1) and found it to be quite adequate.

The average linear strain  $\eta$  on the circular foil membrane as calculated by Dresner for normal incidence of the shock wave is given by

$$\eta = 1.8(h/D)^2 \quad . \quad (2)$$

The stress-strain curve for the foil can be determined using Eqs. (1) and (2) by exposing the foil to a shock and measuring  $P$  and  $h$ . Conversely, if the stress-strain curve is known, the pressure as a function of  $h$  can be calculated:

$$P = 7.25 \frac{T}{D^2} h \sigma \quad . \quad (3)$$

For large  $\eta$ ,  $\sigma$  is nearly constant and  $P$  is nearly linear in  $h$ .

Consider now the dependence of Eqs. (1) and (3) upon the shock pulse duration. Recall that Eq. (1) was derived for a square pulse of infinite duration and infinitesimal risetime. The pertinent time in the problem is that time required to deform the foil, and is of the order of 60  $\mu$ sec for 1-inch-diameter membranes. The infinitesimal risetime approximation is good since the risetime of a high pressure shock wave is much less than the deformation time and independent of the metallic membrane material for a given stress in the region of plastic deformation. The time duration of the shock pulses in the calibration experiments (see Section III) was from 2 to 12  $\mu$ sec, and was for all practical purposes of infinite duration as compared to the distortion time. The time duration of most shock phenomena is also much greater than the membrane response time and the former can be approximated by a pulse of infinite duration. Thus the permanent deformation of the membrane will not depend upon the decay shape for single-step air shocks.

The deformation  $h$  is independent of the shock wave's shape and duration for an additional reason. Dresner<sup>2</sup> has shown that the maximum

strain for an elastic membrane is about 2.3 times greater for sudden application of pressure than for a slowly increasing pressure, where again the pertinent time is the response time of the membrane ( $\sim 60 \mu\text{sec}$ ). Thus because of the greater strain for sudden pulses, if the membrane is not ruptured by the sudden shock (of pressure  $P$ ) it will not be ruptured by the long decaying component of the shock pulse, independent of the duration or shape of the latter.

As a consequence of the above effect the relevant pressure in Eq. (3) is the maximum peak overpressure  $P$ , which is precisely what one normally wishes to measure. Experiments have verified that  $h$  is determined by  $P$  and not by the pulse shape for single-step air shocks (see Section III).

### III. CALIBRATION OF FOIL MEMBRANES

Experiments<sup>\*</sup> using a shock tube were performed in order to determine the pressure  $P$  as a function of the permanent maximum deformation  $h$  for various diameter  $D$  and thickness  $T$ . Once  $P$  as a function of  $h$  is found, it is then possible to use Eqs. (1) and (2) to determine the stress-strain curve for the particular aluminum foil used. Finally, once the stress-strain curve is determined for a particular  $T$ , one can calculate  $P$  as a function of  $h$  for any  $D$ .

One must use caution in relating data from completely different foil "batches" even though  $T$  may be the same; the stress-strain curves of different "batches" can differ due to differences in work hardening. (Consequently, in this study all membranes of the same  $T$  were made from the same roll of aluminum foil.)

The experimental setup was as follows. Membranes (two for each shock wave shot) were mounted in the side of the shock tube<sup>3</sup> so that the shock wave was tangentially incident upon them. The membranes were also kept far from the open end of the shock tube in order to minimize the effect of end reflections. The peak shock overpressure was measured using Kistler Model 603A pressure transducers. Since the shock wave was incident tangentially upon the membrane,  $P$  in Eqs. (1) and (3) is the peak incident overpressure, and not a reflected overpressure. For low shock overpressures,

---

<sup>\*</sup>The authors gratefully acknowledge the experimental assistance of C. B. Brooks.

the driver of the shock tube was filled with compressed air, while higher overpressures were obtained by exploding a propane-oxygen mixture in the driver.<sup>3</sup> After the shot, the permanent deformation  $h$  can easily be seen and can be measured from either side of the membrane plate after disassembly. With an optical micrometer,  $h$  can be measured to  $\pm 0.002$  inch without difficulty. The point of maximum deflection (which will not be at the center of the membrane since the shock wave is tangential) can be found by visual inspection. The shadow from side illumination is a great aid in locating the point of maximum deflection, which can be marked with a felt-tipped pen. The edge of the membrane can be used for a zero deflection reference point.

The stress-strain curve for each  $T$  was calculated from the data by using Eqs. (1) and (2). No dependence upon  $D$  was found as will be shown below. Figure 1 shows the stress-strain curve for aluminum with  $T = 5$  mils. Figure 2 shows the data for both the 5-mil and 1-mil foil. The experimental points for various  $D$  have been plotted with different symbols in Fig. 2. There was no dependence upon  $D$  in the stress-strain curve thus indicating that Eqs. (1) and (2) have the correct  $D$  dependence. Therefore the data for all  $D$  can be combined to give a better determination of  $\sigma$  as a function of  $\eta$ . For a given strain, the stress was about 10% less in the 5-mil foil than in the 1-mil foil. Consequently a reasonable estimate of  $\sigma$  (and thus  $P$ ) can be made without additional experimental calibrations by using the average stress-strain curve. However, in order to avoid uncertainties due to differences in work hardening, each foil batch should be calibrated. Otherwise deviations of approximately 10% in the stress for constant strain may occur, as illustrated by the differences between the 1-mil and the 5-mil foil stress-strain curves. Note that  $\sigma$  is nearly constant for large  $\eta$ , confirming the reasonableness of the constant stress approximation in the plastic region in the derivation of Eq. (1).

Figures 3 and 4 show  $P$  as a function of  $h$  for several  $D$  for foil of thickness 5 mils and 1 mil respectively. The plotted points are experimental values as determined directly from the shock tube measurements while the curves are theoretical values as calculated from the experimentally determined stress-strain curves and using Eqs. (2) and (3).

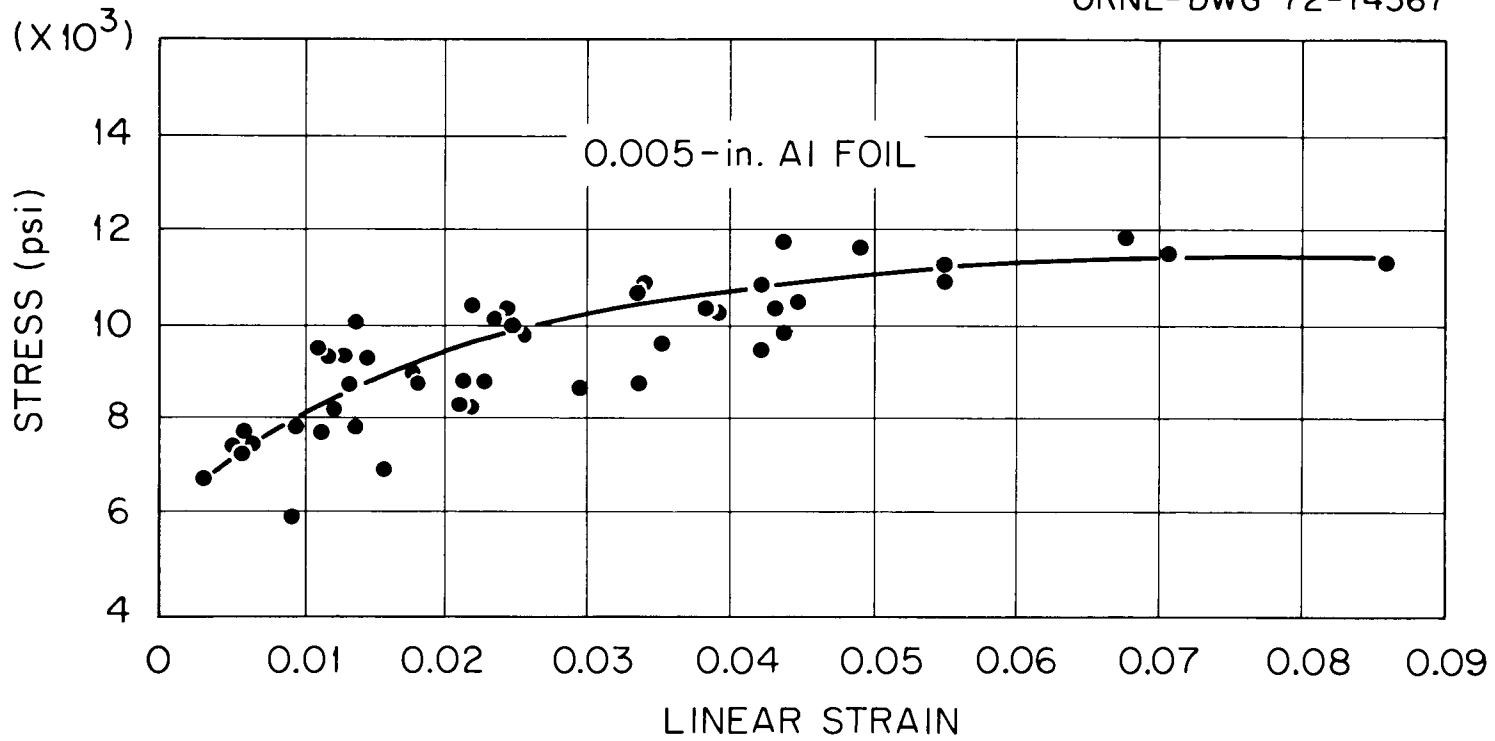


Fig. 1. Stress-strain curve for 0.005-inch-thick aluminum foil.

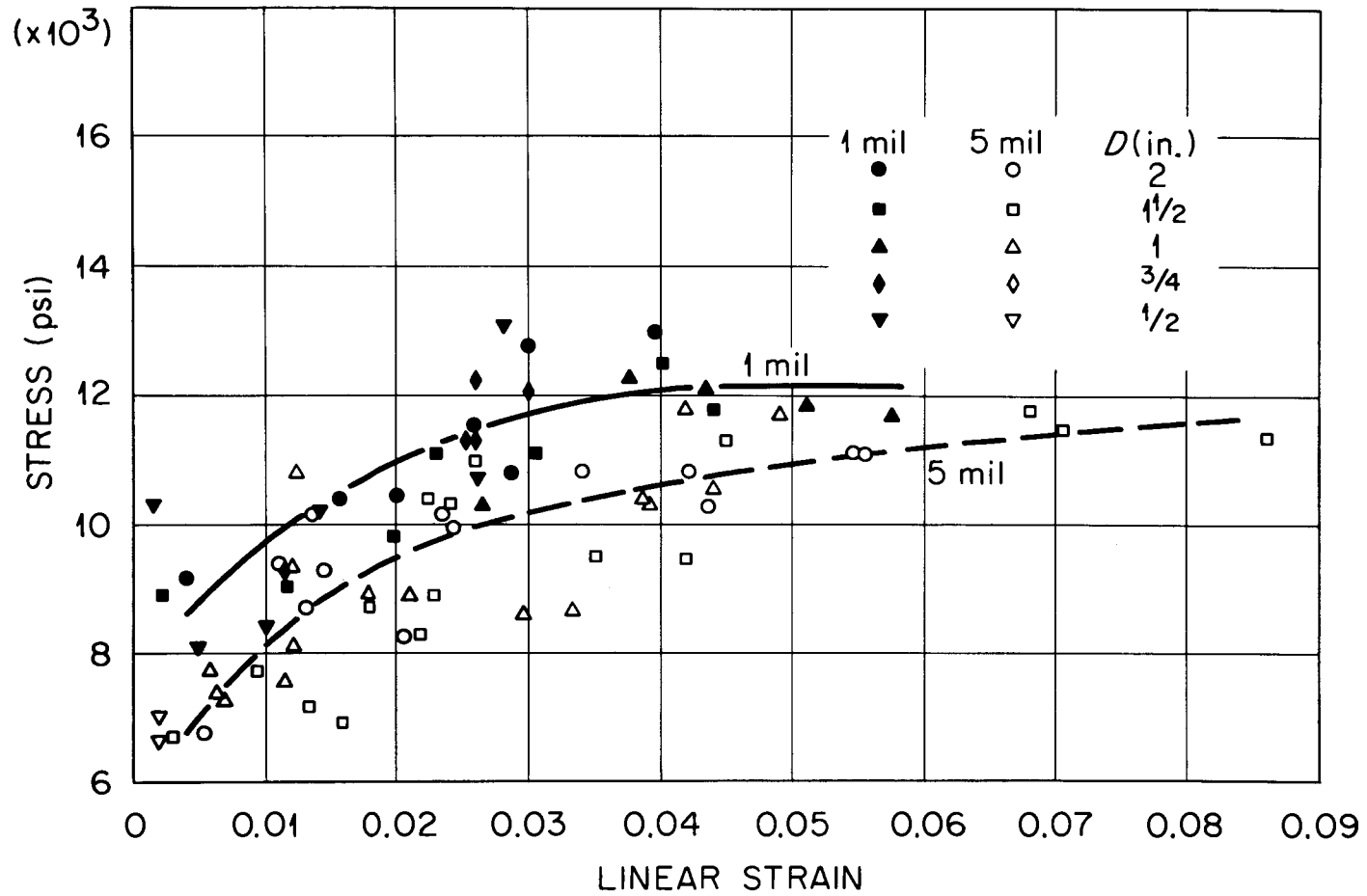


Fig. 2. Stress-strain curves for 0.005- and 0.001-inch-thick aluminum foil.

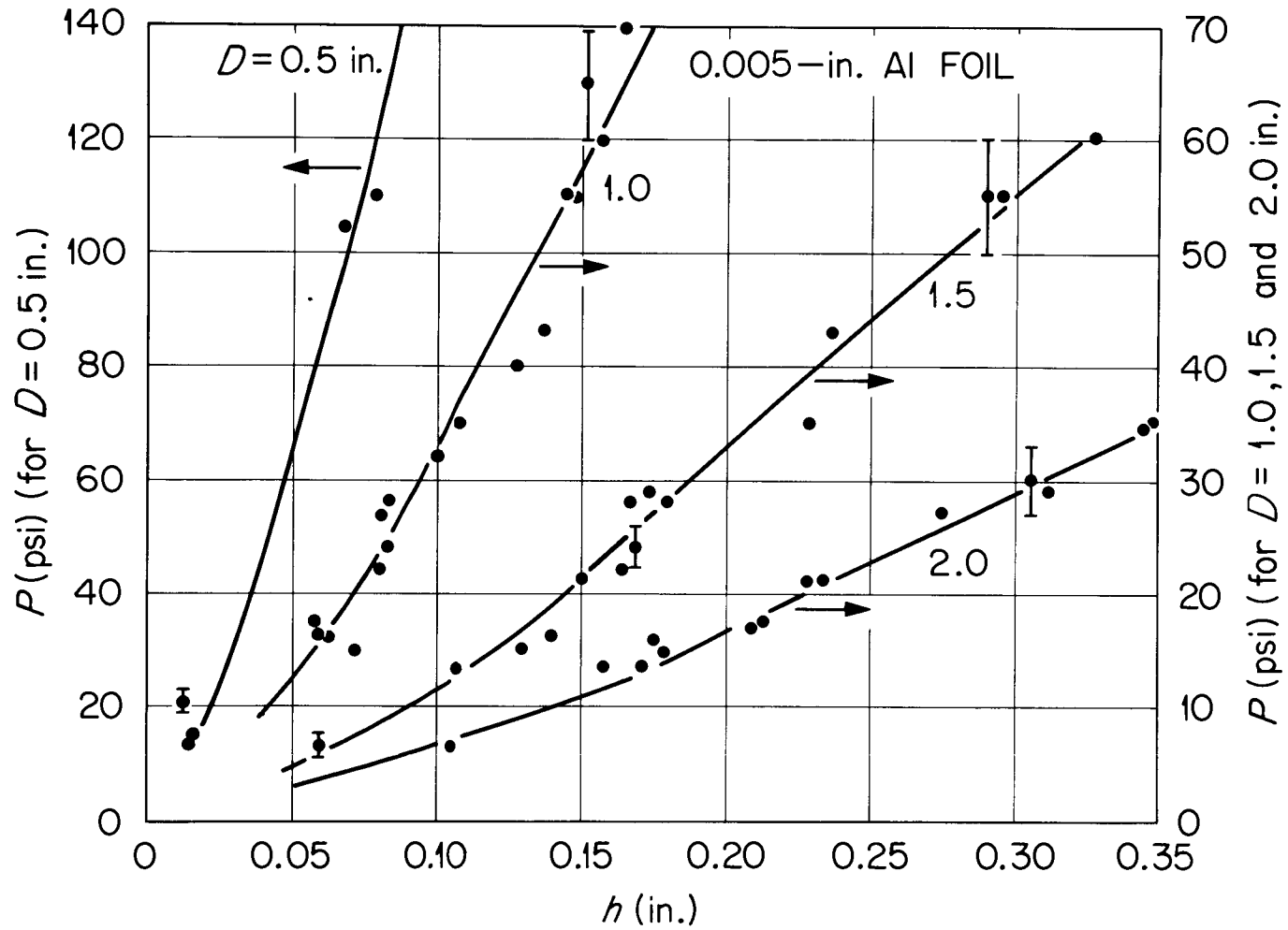


Fig. 3. Pressure as a function of permanent deformation for 0.005-inch-thick aluminum foil.

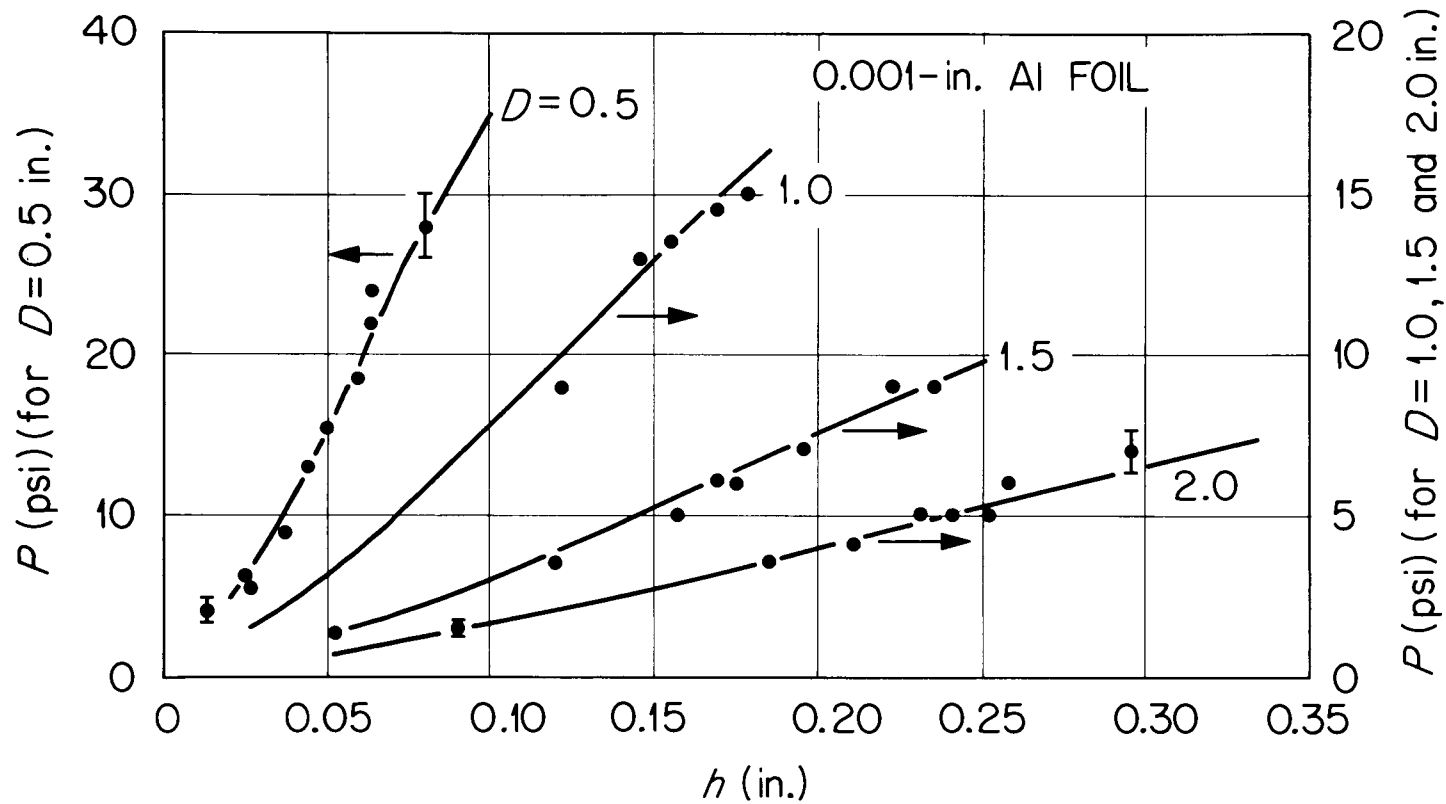


Fig. 4. Pressure as a function of permanent deformation for 0.001-inch-thick aluminum foil.

The curves start and terminate at the region where the strain is beyond the elastic region and at the approximate point of rupture, respectively. The thicker foil ruptured at a greater  $\eta_{\max}$  than the thinner foil.

It is desirable to first determine the stress-strain curve and then to calculate P from Eqs. (2) and (3) using the stress-strain curve for each desired D. The effect of spurious deflections is then minimized on the curves giving P as a function of h. Such spurious deflections can occur, for instance, if there is a local flaw in the foil membrane. Because of such deflections, it is also desirable to have several membranes of the same D in each gauge exposed to the pressure. Thus one first experimentally determines  $\sigma(\eta)$  as in Fig. 1. Then the pressure curves for each diameter D can be drawn from the stress-strain curve and Eqs. (2) and (3) as shown in Fig. 3.

Figure 5 shows typical shock wave pulse shapes incident upon the foil. In agreement with the expectation discussed in the previous section, no dependence of Eq. (3) upon the pulse shape or duration was detected.

For slowly traveling shock waves the constant in Eq. (2) can differ for normal and tangential incidence of the shock wave, i.e., for different geometries. Dresner<sup>2</sup> has shown that for an infinite ribbon, normal and tangential shock incidence give the same strain when the pressure velocity exceeds the signal velocity in the membrane. But when the signal velocity exceeds the pressure velocity, the maximum strain in the membrane will differ for the two cases by a simple factor. However such a modification will not affect the calibration since it only scales the stress-strain curve, providing that one uses the same geometry in calibration as is to be used in the overpressure measurements. (We have designed the gauges for tangential incidence for practical reasons as explained in Section IV.)

Furthermore, Eq. (2) was derived from the membrane's permanently deformed envelope shape resulting from normal shock wave incidence.<sup>1</sup> The deformed shape of the membrane for a tangentially incident shock curve will differ somewhat, primarily by being asymmetrical, with the maximum deformation somewhat "downwind" from the membrane's center. Thus the

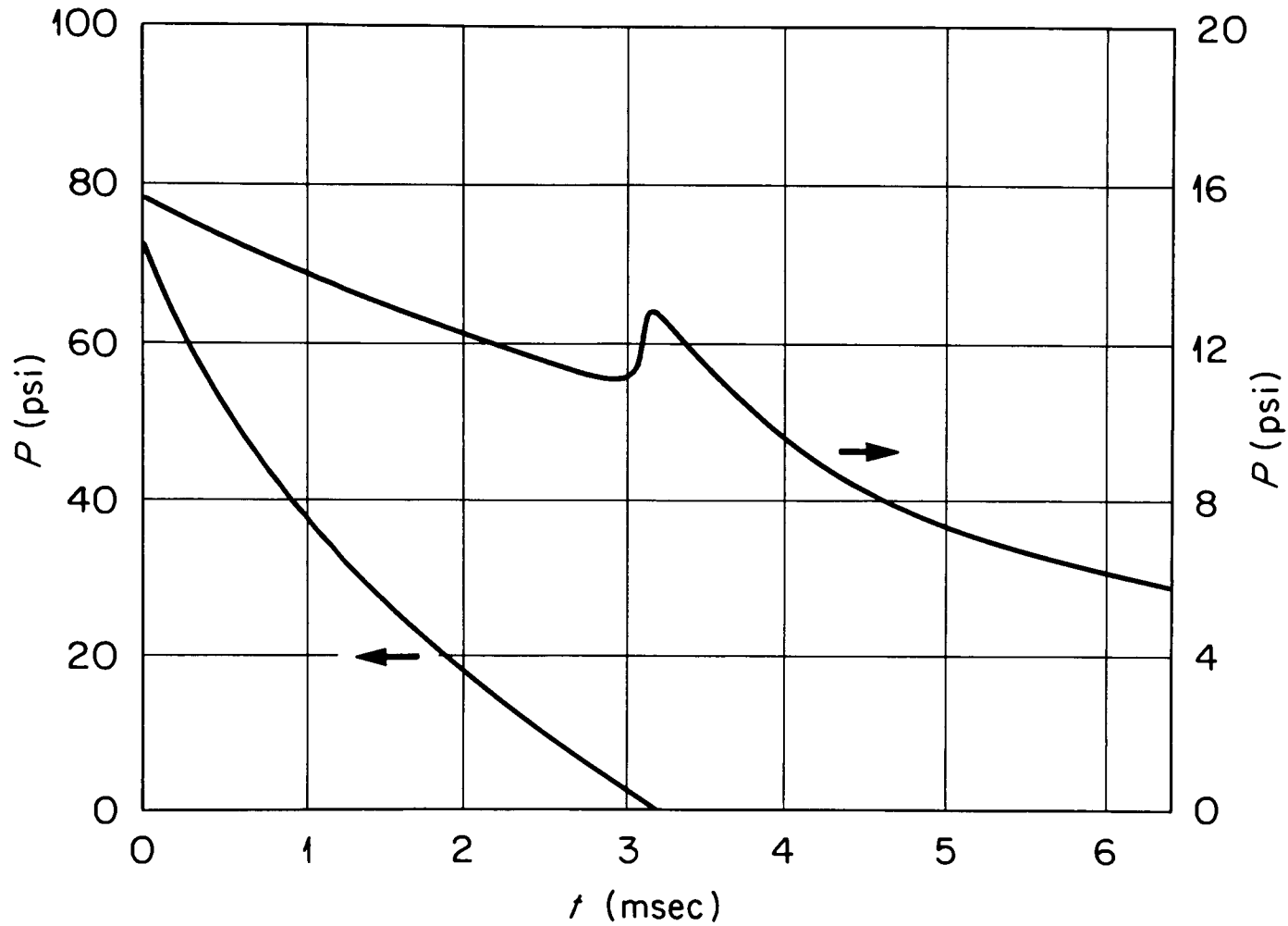


Fig. 5. Pressure as a function of time curves for short and long duration shock tube pulses.

average linear strain as calculated by Eq. (2) will differ somewhat from the average linear strain for tangential incidence. However, the calibrations will not be greatly affected since the strain for the calibration and experimental field tests were calculated in the same manner. No effect was in fact observed.

#### IV. THE DESIGN OF THE GAUGE

##### A. General Description

The pressure gauge was designed for low cost and ease of fabrication. No electronic equipment of any kind is needed in the operation of the gauge. A typical gauge is shown side-on in Fig. 6, and Fig. 7 shows the assembled gauge and a smaller (6" steel pipe) gauge.

The topmost protective plate prevents debris accelerated by the blast from puncturing the foil membranes, and it also assures that the shock wave is incident tangentially upon the membranes. The aluminum foil is sandwiched between 1/4- and 1/8-inch plates; it is secured to the 1/4-inch plate with an epoxy adhesive. Great care must be taken to prevent any adhesive from flowing onto the membrane during cementing, for the effective diameter  $D$  would then be reduced. The large pipe chamber is sealed. However a very small hole into the pipe chamber should be left in order to allow for barometric and temperature changes. Such a hole was not included in the design of our original gauges.

Figure 8 shows a typical membrane plate (with membranes of  $D = 2$ ,  $1-1/2$ ,  $1$ ,  $3/4$ , and  $1/2$  inches). The membranes should not be precurved significantly since precurving reduces the strain for a given pressure and the calibration would therefore be quite different.

Figure 9 shows a gauge positioned in order to measure the overpressure close to the ground surface. Figures 10 and 11 show the top and bottom view of a membrane plate with 0.005-inch aluminum foil membranes after exposure to approximately 15 psi. In some environments the spacing between the protective plate and membrane may be filled with debris and dirt, but  $h$  can then be measured from the chamber side of the membrane. Since

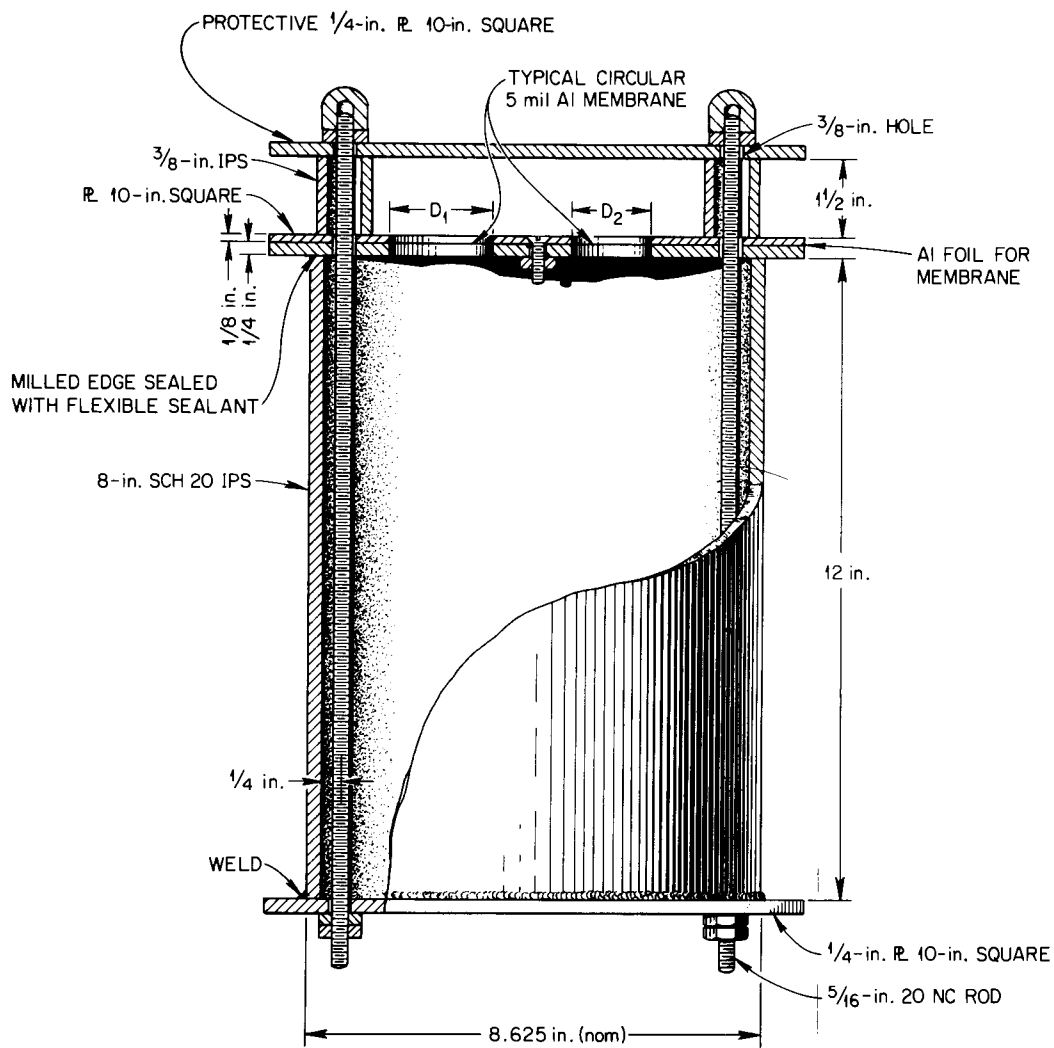


Fig. 6. Mechanical drawing (side view) of pressure gauge.



Fig. 7. Assembled gauge of the dimensions given in Fig. 6, and a smaller (6-in.) gauge shown partially disassembled.

PHOTO 3977-72

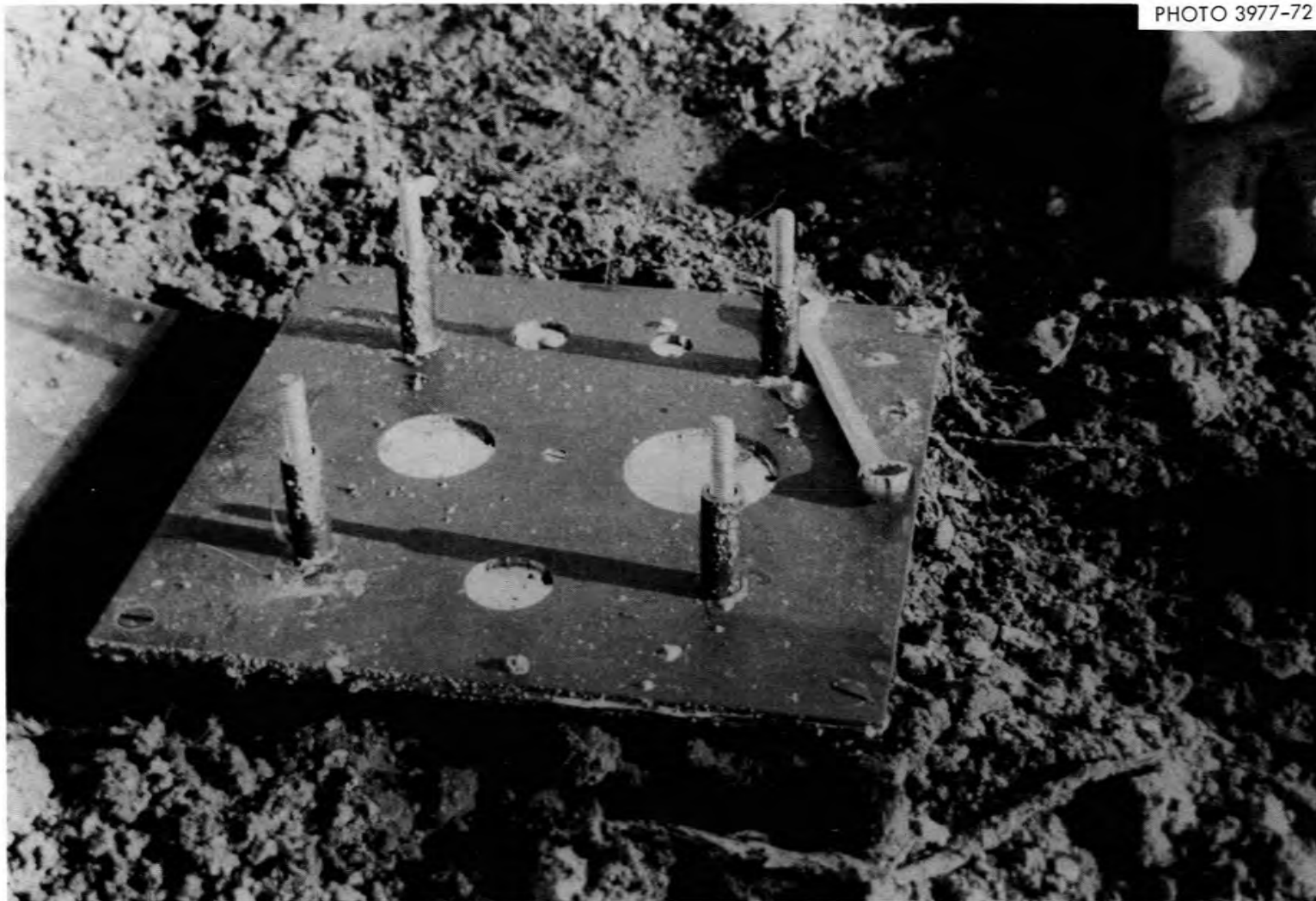


Fig. 8. Pressure gauge mounted to measure the ground-surface overpressure with protective plate removed.

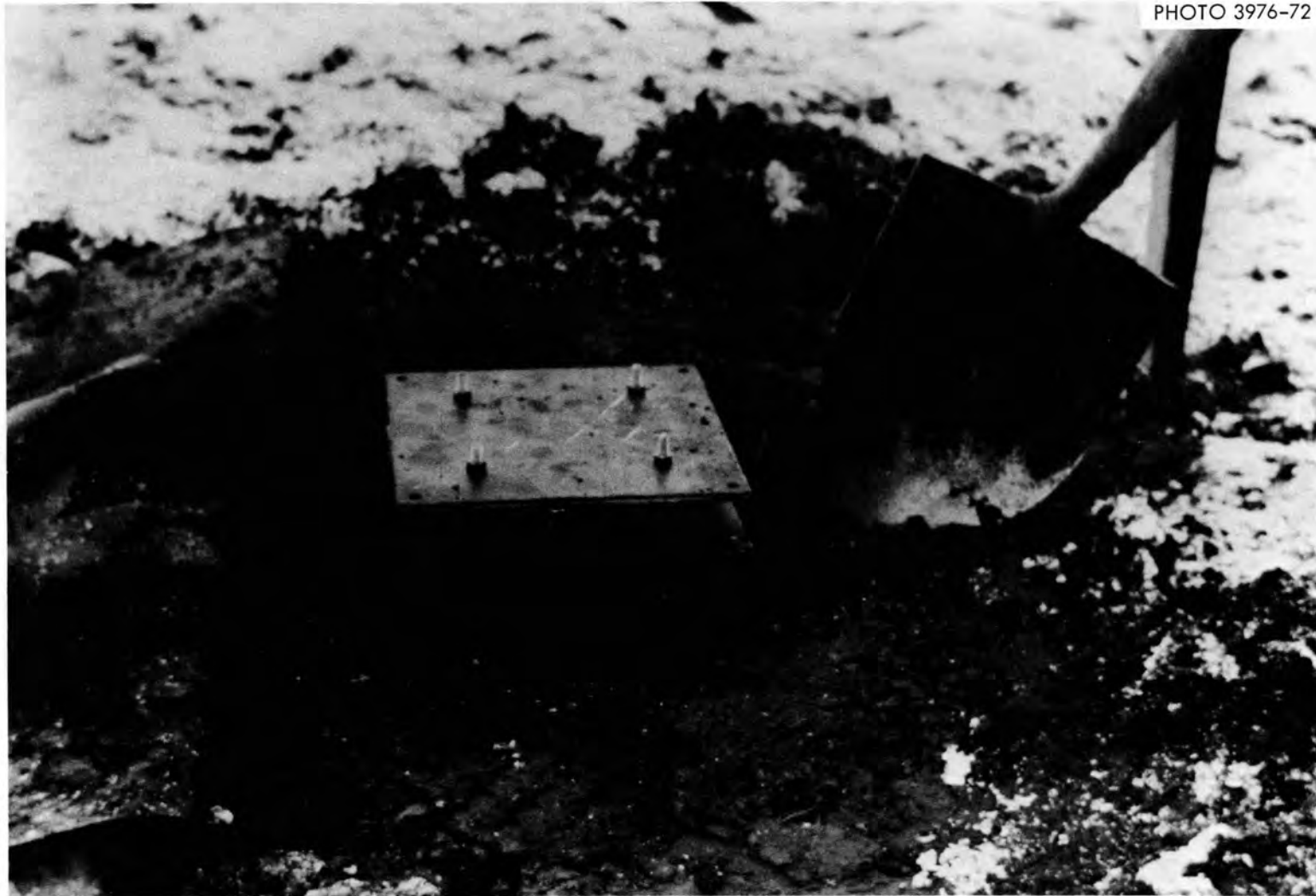


Fig. 9. Pressure gauge mounted to measure the ground-surface overpressure with protective plate in place.

PHOTO 3983-72



Fig. 10. Top view of membrane plate with 0.005-inch-thick foils after subjection to 15 psi nominal overpressure.

PHOTO 3981-72

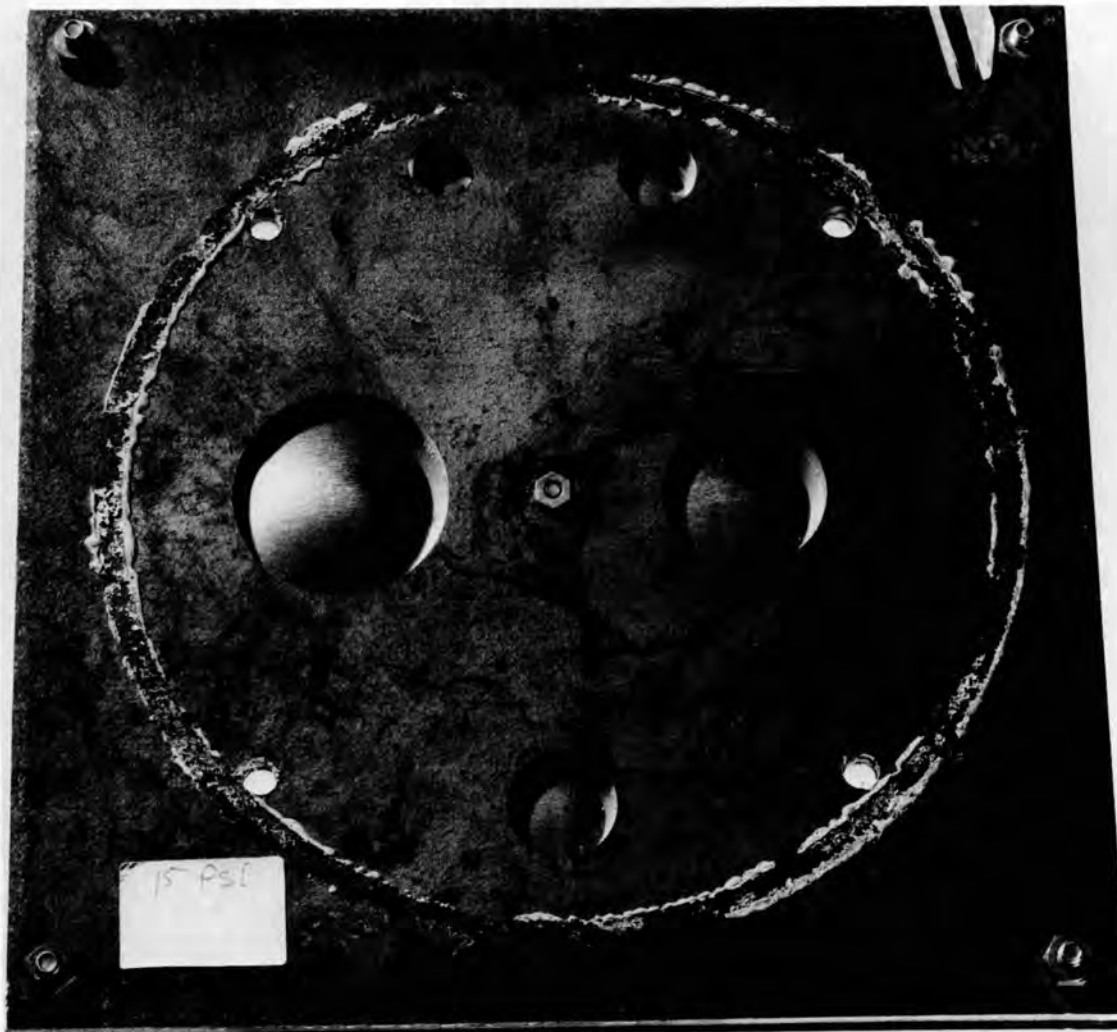


Fig. 11. Bottom view of membrane plate with 0.005-inch-thick foil after subjection to 15 psi nominal overpressure.

the debris arrives after the shock, it will not affect the measured peak pressure. Also since the velocity of the debris is tangential to the membrane, the membrane should not be significantly deformed by the impact of such debris. The membrane plates can be dismantled and removed to another location for measurement as long as care is taken not to deform the membranes.

B. Choosing D and T

Both D and T should be chosen in order that a reasonable deformation  $h$  will result when the gauge is subjected to the pressures expected in the experimental environment. The average linear strain  $\eta$  should be neither in the elastic region nor too close to the point of rupture of the stress-strain curve of the particular foil used. These limits upon  $\eta$  can be determined approximately from the stress-strain curve (see Section V). For example, if the expected pressure  $P$  is in the region  $P_1 < P < P_2$ , several different diameters should be chosen for a reasonable  $T$  such that the largest (smallest)  $D$  would record  $P_1(P_2)$  satisfactorily. If  $D$  is much less than 1/2 inch, edge effects become uncertain; if  $D$  is much greater than 2 inches, the membranes are more easily damaged. These limits upon  $D$  will determine a reasonable  $T$ . It is important to provide several membranes of the same  $D$  (per plate) since spurious deformations can then be identified with the multiple readings.

Field tests and theoretical considerations indicate the desirability of positioning the larger diameter membranes on one side of the gauge plate so that the larger diameter membranes should be "downwind" to the shock. Then if the larger diameter membranes should rupture, the smaller diameter "upwind" membranes would not be affected by the rush of air into the pipe chamber. They will already have been deformed since it takes about 60  $\mu$ sec for a 1-inch-diameter foil to deform, while a 50 psi shock wave will take about 150  $\mu$ sec to travel 2 inches. (Our original gauges did not have the membranes arranged in this manner; however, the overpressure at the experimental field tests were insufficient to rupture the membranes.)

The curves in Figs. 1 through 4 combined with Eqs. (1) through (3) can be used to estimate the desired D and T for other experimental situations. Again the stress-strain curves in Fig. 2 should give a reasonable estimate of P.

### C. Other Membrane Gauges

#### Foil Meters

In Operation Greenhouse<sup>5</sup> in 1951, Ballistic Research Laboratories used a foil rupture gauge to measure head-on blast pressure in the low hundred psi range. The gauge was machined in a massive steel plate set in a concrete wall normal to the blast wind. Aluminum foil a few mils thick was held in an elaborate mechanical clamp. Unsupported circles of varying diameter provided the range of pressure intervals. Rupture pressure was calibrated in a shock tube. The gauge had the disadvantages of providing only discontinuous pressure intervals and of great expense due to the machining required.

#### German Gauges

At Operation Plumbbob,<sup>6</sup> the German experimental program tested two types of mechanical pressure gauges. One type consisted of 18 membranes of various diameters made from paper which would fail at different pressures. A second type of mechanical gauge consisted of a vibrating metal circular membrane which was in contact with a small pin at the membrane's center. The pressure was then recorded by the displacement of the small pin caused by the elastic vibrations of the membrane when subjected to shock.

The paper membranes have the disadvantage that they do not provide a continuous scale to measure the pressure. The paper would also be susceptible to humidity effects and water damage.

The design of the German metal membrane gauges was based upon the elastic (not plastic) deformation of the metal membrane and was therefore based upon a completely different principle than the CRNL gauges. The German gauges have several disadvantages. Firstly, their design is much

more complex and would be more expensive to fabricate, and secondly, calibration problems could arise due to both the inertia and complications from friction of the small pin. The final report of the German gauges is not available so a complete evaluation could not be made.

#### V. THE EXPERIMENTAL FIELD RESULTS

Fourteen aluminum foil pressure gauges have been tested at the MIXED COMPANY Event, a detonation<sup>4</sup> of 500 tons of TNT on November 13, 1972. The gauges were placed at predicted pressures ranging from 5 to 100 psi, and in two cases, in the immediate vicinity of standard transducer gauges\* so that the technique could be compared to standard methods.

Five gauges (Nos. 1 through 5) were constructed from 8-IN SCH20 IPS pipe, with the membrane configuration shown in Figs. 10 and 11. Three gauges (Nos. 6 through 8) were constructed from 6-IN SCH20 IPS pipe, with three each of 1/2-, 3/8- and 1/4-inch-diameter membranes with  $T = 0.005$  inch.

Table I shows the pressure readings for low pressure as measured at the MIXED COMPANY detonation. The uncertainty,  $\Delta P$ , of the measured pressure as given in Table I (for  $D = 2$  inches and  $D = 1/2$  inch) is determined from the uncertainty in the stress-strain curve and from the error in measuring  $h$ . The uncertainty,  $\Delta P$ , does not include any estimate of the anomalous deformations which occasionally occur. Such deformations were eliminated by the following procedure. Each gauge had 5 membranes. If a pressure reading deviated by more than  $2\Delta P$  from the other readings of the same gauge, it was considered to be a spurious reading and was not used in calculating the average pressure as listed. The reasonableness of this procedure to eliminate spurious readings is illustrated in the shock tube measurements. Approximately

---

\*The comparative transducer overpressure measurements were made possible by the cooperation of Captain James Dick of the Air Force Weapons Laboratory and T. E. Kennedy and J. W. Ball of the U.S. Army Engineer Waterways Experiment Station.

TABLE I. Overpressure data as determined from low pressure gauges.  
A transducer reading from Ref. 8 is given for comparison.

Gauge No.	Diameter of Membrane (Inches)					Gauge Average <sup>a</sup> (psi)	Location From GZ		Transducer Reading
	2	1-1/2	1	3/4	1/2		Distance	Azimuth	
T = 0.005 Inch									
1	30.1 ± 2.4	37.8 <sup>b</sup>	29.3	28.5	28.4 ± 2.6	29.1 ± 2.5	645 ft	110°	---
2	16.7 ± 1.4	14.5	19.0	20.1	26.0 ± 2.5 <sup>c</sup>	16.7 ± 1.5	840 ft	109°	---
3	13.5 ± 1.1	14.5	17.5	14.5 <sup>c</sup>	13.0 ± 1.2 <sup>c</sup>	15.2 ± 1.3	860 ft	269°	14.3 ± 1.4 <sup>d</sup>
4	12.7 ± 1.0	12.7	12.5	15.0 <sup>c</sup>	---	12.6 ± 1.0	1000 ft	108°	---
T = 0.001 Inch									
5	4.2 ± 0.4 <sup>e</sup>	4.6 <sup>e</sup>	5.0	7.2 <sup>c</sup>	6.0 ± 0.6 <sup>c</sup>	5.0 ± 0.5	1430 ft	113°	---

<sup>a</sup>Points with b), c) or e) footnotes were not included.

<sup>b</sup>Anomolously high or low; not included in calculating the average gauge pressure.

<sup>c</sup>Too close to elastic region or point of rupture; therefore not included in calculating the average gauge pressure.

<sup>d</sup>From Ref. 8; preliminary measurement at same azimuth and distance.

<sup>e</sup>Foil damaged before measurement due to rough handling; resultant measurement probably low.

75 membranes were tested and about 5% of the readings gave poor pressure measurements. When several membranes are simultaneously exposed to the shock wave, the spurious readings are quite apparent, and usually differ by several  $\Delta P$ . In Table I, only one pressure reading was spurious, and it deviated by more than  $3\Delta P$ . The pressure at a particular location can be determined to an accuracy of about 10% by the above technique, providing that the gauge has several membranes.

Table II shows the pressure readings as measured at higher pressure. The data was analyzed in the same manner as described above. The high pressure measurements would have been improved if the diameters of the membranes had been larger; it was found that the 1/4-inch-membranes were too small to give good measurements. The overpressures were insufficient to rupture any membranes. Typical  $\Delta P$ 's are shown. Two of the three spurious pressure readings deviated from the average by more than  $4\Delta P$ . The increased percentage of spurious readings, as compared to the low pressure gauge tests and the shock tube tests, may be the result of using membranes of too small diameters.

Two gauges were placed near standard transducer-type gauges; one at an azimuth of  $160^\circ$  from ground zero, near Air Force Weapons Laboratory<sup>7</sup> (AFWL) gauges on the  $135^\circ$  azimuth, and a second adjacent to an Army Engineers<sup>8</sup> gauge on the  $270^\circ$  azimuth. Figure 12 shows the ORNL foil membrane gauge results, as well as AFWL<sup>7</sup> preliminary transducer gauge readings on the  $135^\circ$  azimuth, the Army Engineers<sup>8</sup> transducer gauge reading adjacent to ORNL gauge No. 3, and the theoretical predicted pressure versus range curve. The agreement of the measurements is very good, with all accepted readings being well within the experimental errors. The predicted pressure-distance calculations<sup>4</sup> seem to overestimate the pressure at distances in the neighborhood of 400 feet from ground zero and along these three azimuths. It should be remembered that the membrane pressure gauge's cost is about 2% of that of a channel of the transducer gauge system used in a large outdoor blast test of this type.

A large negative phase pulse can cause difficulties, since the pipe chamber is at atmospheric pressure and the membrane will tend to

Table II. Overpressure data as determined from the high pressure gauges. A transducer reading from Ref. 7 is given for comparison.

Gauge No.	D = 1/2 Inch Readings				D = 3/8 Inch Readings			Gauge Average <sup>a</sup>	Location from GZ		Transducer Reading
	-	-	-	-	psi	-	-		-	Distance	
6	68 ± 6	63	54 <sup>b</sup>		67 ± 7	61		64.8 ± 5.3	420 ft	104°	
7	42 ± 4	39	35		31 ± 3	29	20 <sup>b</sup>	35.2 ± 2.9	540 ft	105°	
8	67 ± 6	59	44		54 ± 6	46	23 <sup>b</sup>	54.0 ± 5.0	503 ft	160°	50 ± 5 <sup>c</sup>

<sup>a</sup>Points with footnote (b) were not included in average.

<sup>b</sup>Anomolously high or low; not included in calculating the average gauge pressure.

<sup>c</sup>From Ref. 7; preliminary measurement by interpolation from gauges on an azimuth of 135° from ground zero and at nearly the same range from ground zero as gauge No. 8.



deflect outward during the negative phase. However, since the gauge is sealed, the negative phase pressure difference will be very small as compared to the initial overpressure, and the former will not further deform the membrane. But if  $D$  is very large and  $T$  small ( $\sim 1$  mil), the negative phase may fold the membranes back out and crease the foil. However, if the foil is not too badly wrinkled, it can be smoothed to approximately its original positive phase deformation and  $h$  then measured. The duration of the negative phase is irrelevant.

A limitation of this method is its unreliability for recording a slowly-rising overpressure (longer than  $60 \mu\text{sec}$ ), such as may occur inside a blast shelter with a small opening to the outside. Inaccurate readings can also result from multiple-step air shocks.

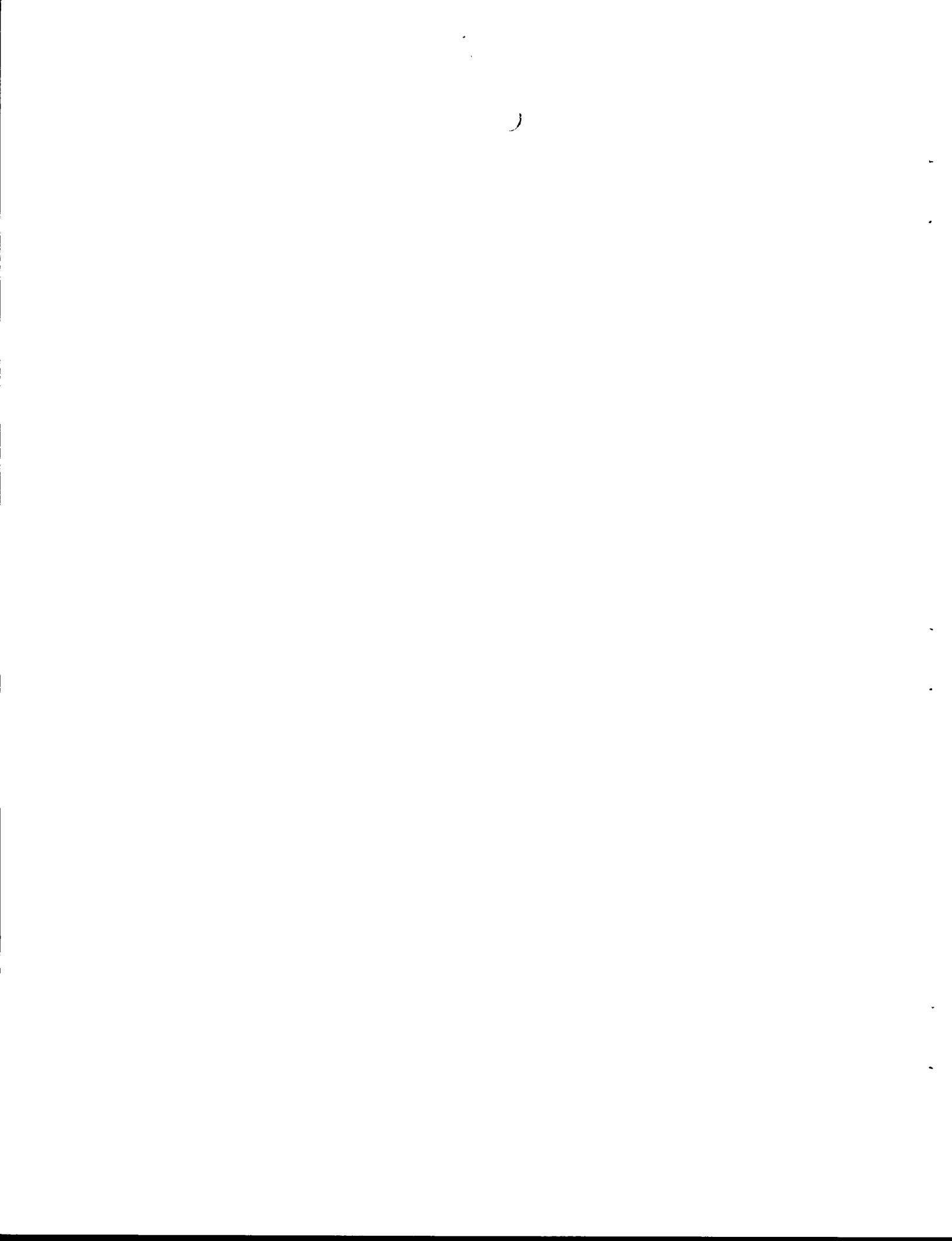
## VI. CONCLUSIONS AND RECOMMENDATIONS

This thin-foil pressure gauge is both a simple and inexpensive device, yet it is reliable for measuring peak positive-phase shock overpressures and can be designed to measure pressures from a few psi to hundreds of psi to an accuracy of  $\pm 10\%$ . The gauge design was successfully tested in a realistic experimental environment. The recorded overpressures agreed well with those obtained from standard electronic transducer gauges.

This gauge should be designed with multiple membranes having diameters ranging between  $1/2$  and 2 inches. The stress-strain calibration curves given in this report can be used to make a reasonable estimate of the calibration for gauges with aluminum-foil membranes of similar  $T$  and  $D$ , provided that the shock wave is tangentially incident upon circular membranes. However, in order to avoid uncertainties due to differences in work hardening, each foil batch should be calibrated using the described shock tube technique.

REFERENCES

1. L. Dresner, "Plastic Deformation of Circular Foils Under Shock Loading," ORNL-TM-2485 (1969).
2. L. Dresner, Jour. Applied Phys. 41, 2542 (1970).
3. L. Dresner and C. V. Chester, "A Four-Inch Shock Tube Driven by an Exploding Gas Mixture," ORNL-TM-2094 (1968).
4. Middle North Series, MIXED COMPANY Event, Technical and Administrative Document, Defense Nuclear Agency, Kirtland Air Force Base (April 1972).
5. Julius J. Meszaros, "Determination of Mach-Region Peak Blast Pressure with Foil Meters," Operation Greenhouse, Scientific Directors Report WT-55, Annex 1.6 Part III, Section 2, Ballistic Research Laboratories, Aberdeen, Maryland (December 1951).
6. Operation Plumbbob, Test of German Underground Personnel Shelters, WT-1454 (1962). Additional information concerning the German gauges was provided by Ammann & Whitney, New York, New York.
7. Air Force Weapons Laboratory, Kirtland Air Force Base, New Mexico, private communication.
8. U.S. Army Engineer Waterways Experiment Station, Corps of Engineers, Vicksburg, Mississippi, private communication.



INTERNAL DISTRIBUTION

- |   |                        |
|---|------------------------|
| 1. Biology Library  | 80. C. B. Brooks       |
| 2-4. Central Research Library                                   | 81. C. V. Chester      |
| 5-54. Civil Defense Research Section<br>Library                 | 82. G. A. Cristy       |
| 55. MIT Practice School   | 83. F. L. Culler       |
| 56. ORNL - Y-12 Technical Library<br>Document Reference Section | 84. L. Dresner         |
| 57-76. Laboratory Records Department                            | 85. R. F. Hibbs        |
| 77. Laboratory Records, ORNL R.C.                               | 86-87. C. H. Kearny    |
| 78. ORNL Patent Office  | 88-89. M. W. Manweiler |
| 79. J. A. Auxier  | 90. J. R. Totter       |
|   | 91. A. M. Weinberg     |
|   | 92. E. P. Wigner       |

EXTERNAL DISTRIBUTION

- 93. Director, Admiralty Surface Weapons Establishment, Ministry of Defense, ATTN: D. S. G. Mullens, Pottsgdown Cosham Portsmouth P06 4AA, United Kingdom
- 94. Commanding Officer, Air Force Cambridge Research Lab., ATTN: LWW, E. E. Bliamptis, Bedford, MA 01730
- 95. Headquarters, Air Force Systems Command, ATTN: Lt. Col. J. Choromokos, Andrews AFB, MD 20331
- 96-104. Director, Air Force Weapons Laboratory, ATTN: SYT, Capt. D. A. Matuska, DEV, Maj. H. Pahl, Capt. J. Dick, DEV-F, J. Bratton, Capt. S. P. Chisholm, DEV-G, Maj. N. E. Lamping, R. Bunker, Lt. W. H. Kruger, J. Repichowski, Kirtland AFB, NM 87117
- 105-106. Atmospheric Sciences Laboratory, U.S. Army Electronic Command, ATTN: R. Robbiani, AMSEL-TL-NS, R. A. Freiberg, Fort Monmouth, NJ 07703
- 107-111. Commanding Officer, Ballistic Research Laboratory, ATTN: G. D. Teel, R. Mayerhofer, R. Schumacher, N. H. Ethridge, W. J. Schuman, Aberdeen Proving Ground, MD 21005
- 112. Director-General, Defence Research Establishment, ATTN: B. R. Long, Suffield, Ralston, Alberta, Canada
- 113. Defense Civil Preparedness Agency, ATTN: Donald A. Bettge, Room 1D538, The Pentagon, Washington, D.C. 20301
- 114. Defense Civil Preparedness Agency, ATTN: George N. Sission, Room 1D538, The Pentagon, Washington, D.C. 20301
- 115. Commander, Field Command, Defense Nuclear Agency, ATTN: FCTD, FCTD-T, Kirtland AFB, NM 87115
- 116-118. Director, Defense Nuclear Agency, ATTN: SPLN, J. G. Lewis, J. Kelso, Maj. W. Shepard, Washington, D.C. 20305
- 119. Director, Defense Nuclear Agency, ATTN: SPSS, Maj. R. Waters, Washington, D.C. 20305
- 120. Denver Research Institute, University of Denver, ATTN: J. Wisotski, P. O. Box 10127, Denver, CO 80210
- 121. Headquarters, Edgewood Arsenal, ATTN: SMUEA-TS-TM, R. V. Navin, Edgewood, MD 21010

122. General Electric Tempo (DASIAC), ATTN: W. W. Chan, 816 State Street, Santa Barbara, CA 93102
- 123-124. Lovelace Foundation, ATTN: E. R. Fletcher, D. R. Richmond, 5200 Gibson Blvd, S.E., Albuquerque, NM 87108
125. Meteorology Research Incorporated, ATTN: W. Green, 464 West Woodbury Road, Altadena, CA 91001
126. J. J. Meszaros, Ballistic Research Laboratories, Aberdeen, MD 21005
127. Naval Civil Engineering Lab., CODE L51, ATTN: R. J. Odello, Port Hueneme, CA 93043
128. Commander, Naval Ordnance Lab., ATTN: CODE 241, J. Petes, Silver Spring, MD 20910
129. Naval Ship Research and Development Center, ATTN: Mr. Habib, Bethesda, MD 20034
130. Pan American World Airways, ATTN: A. Montrose, P. O. Box 2057, Jackass Flats, NV 89023
131. J. A. Swartout, Union Carbide Corporation, New York 10017
132. Paul Weidlinger Company, ATTN: W. Baron, 110 E. 59th Street, New York, NY 10017
133. Physics International Company, ATTN: F. Sauer, 2700 Mercer Street, San Leandro, CA 94577
- 134-135. Sandia Laboratories, ATTN: L. Vortman, J. W. Reed, P. O. Box 5800, Kirtland AFB, NM 87115
136. Stanford Research Institute, ATTN: Stan Martin, Menlo Park, CA 94025
137. TRW Systems Group, One Space Park, R1/2178, ATTN: P. Lieberman, Redondo Beach, CA 90278
- 138-146. Waterways Experiment Station, ATTN: T. E. Kennedy, Mr. Rooke, B. L. Carnes, J. D. Day, A. A. Rula, J. P. Balsara, G. Jackson, R. Ballard, L. Ingram, P. O. Box 631, Vicksburg, MS 39180
147. Commanding General, U.S. Army Weapons Lab., ATTN: SWERR-R, B. E. Morris, Rock Island, IL 61201
148. U.S. Atomic Energy Commission, ATTN: W. W. Schroebel, Analysis and Evaluation Branch, DBER, Washington, D.C. 20545
149. U.S. Geological Survey, ATTN: D. Roddy, 601 E. Cedar Street, Flagstaff, AZ 86001
150. Patent Office, AEC, ORO
151. Research and Technical Support Division, AEC, ORO
- 152-317. Given distribution as shown in TID-4500 under Instruments category (25 copies - NTIS)